



Synthesis, characterization and application of pure ceria, pure zinc oxide, ceria zinc oxide nano composite: synergetic effect on photo-catalytic degradation of Amido Black 10B in water

Mohammad Hossein Habibi*, Mosa Fakhrpor

Nanotechnology Laboratory, Department of Chemistry, University of Isfahan, Isfahan, 81746-73441 I.R. Iran, Tel. +98-313-7934914; Fax: +98-313-6689732; emails: habibi@chem.ui.ac.ir (M.H. Habibi), mousafakhrpor1@gmail.com (M. Fakhrpor)

Received 11 April 2016; Accepted 14 July 2016

ABSTRACT

Cerium dioxide (CeO_2), zinc oxide (ZnO) and CeO_2 - ZnO nano-structures were synthesized by co-precipitation technique and the synergetic effect of coupled oxide (CeO_2/ZnO) for photo-catalytic degradation of Amido Black 10B in water was investigated. The synthesized nano-particles were characterized using TG-DTG, FESEM, XRD and DRS for their thermal and physicochemical property. TG-DTG results of the precursors showed three steps of weight loss at 163°C (3%), 204°C (6.6%) and 560°C (21.72%). The crystallite size of the CeO_2 , ZnO and CeO_2/ZnO was calculated using XRD data with an average size of 9.80, 19.65 and 32.21 nm, respectively. The XRD results showed well-crystalline mixed phases of cubic cerium oxide (CeO_2) and hexagonal zinc oxide (ZnO). Pure CeO_2 , ZnO and CeO_2/ZnO nano-composite were tested for their photo-catalytic degradation of Amido Black 10B textile dye in water as an aquatic environmental pollutant. The photo-catalytic reactivity results showed an enhanced photo-catalytic activity of coupled CeO_2/ZnO compared to single oxides. This was related to the synergetic effect of coupled CeO_2/ZnO due to the improved separation of photo-generated electron-hole pairs.

Keywords: Pure CeO_2 ; Pure ZnO ; CeO_2 - ZnO ; Nano-structure; Coupled oxide; Synergetic; Photo-catalytic reactivity; Amido Black 10B; Textile dye; Environmental pollutant

1. Introduction

Spinel metal oxide as advanced materials have become an important area of research for their potential advantages and applications [1]. The composite of metal oxides could promote the separation of photo-induced charge carriers [2–4]. Among metal oxides, zinc oxide nanostructures have attracted more attention for their interesting properties and extensive use in a range of applications [5–7]. Cerium (IV) oxide, also known as ceria is a rare earth metal oxide. Ceria have excellent redox properties with many applications in fuel cells, water dissociation and catalytic reactions owing to the redox couple feature of $\text{Ce(III)}/\text{Ce(IV)}$ [8–10]. Binary composites of cerium dioxide have been reported for their

catalytic reactions [11]. Sherly et al. have reported the effect of CeO_2 coupling on the structural, optical and photocatalytic properties of ZnO nanoparticle [12]. Lamba et al. studied the catalytic degradation of direct blue 15 dye and its simulated dye bath effluent under solar light using CeO_2 - ZnO nano-disks [13]. He et al. demonstrated enhanced optical properties of hetero-structured ZnO - CeO_2 nano-composite [14]. Nano-composites are prepared by different synthetic methods using physical and chemical means. The properties of the nano-composites are improved compared to their single counterparts due to the strong surface interactions between the components of nano-composite in binary oxide systems [15]. Zinc oxide and ceria are applied as heterogeneous catalysts for oxidation reactions [16,17]. Reports on the preparation and uses of binary zinc oxide-ceria nano-structures are limited. The Ce(III) and Ce(IV) ions form complex with the

* Corresponding author.

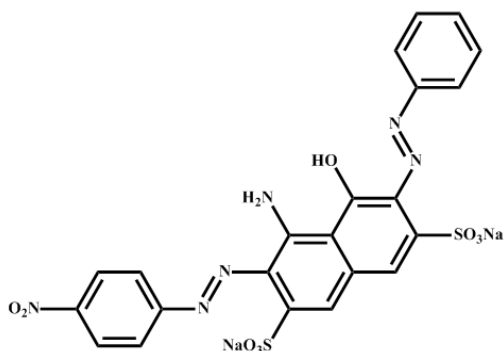


Fig. 1. The structure of Amido Black 10B textile dye as a model of aquatic environmental pollutant.

surface oxygen of ZnO. The presence of redox couple Ce(III)/Ce(IV) could enhance the photocatalytic of the ZnO-CeO₂ nano-composite which act as an electron scavenger and photogenerated electrons in conduction band (CB) of ZnO are transferred to CB of CeO₂ [18,19]. To the best of our knowledge, the preparation of coupled CeO₂-ZnO nano-structures and its synergetic effect of coupled CeO₂-ZnO on photocatalytic degradation of Amido Black 10B in water are not yet reported in the literature.

In this research, coupled CeO₂-ZnO nano-structures (CZN) were synthesized by using co-precipitation technique and fully characterized using TG-DTG, FESEM, XRD and DR. Additionally, the synergetic effect of coupled oxide (CeO₂/ZnO) for photo-catalytic degradation of Amido Black 10B in water was investigated (Fig. 1).

2. Experimental

2.1. Materials

The Amido Black 10B, CeCl₃·7H₂O and ZnCl₂ was purchased from Merck, Germany and used as supplied for the synthesis and application of CeO₂, ZnO and CeO₂-ZnO nano-structures.

2.2. Experimental procedure for preparation of CeO₂, ZnO and CeO₂-ZnO nano-structures

2.2.1. Experimental procedure for preparation of CeO₂ nano-particles

CeO₂ nano-particles were prepared by co-precipitation method from an aqueous solution of CeCl₃·7H₂O. The solution was obtained by dissolving 1.891 g cerium(III) chloride heptahydrate in 50 mL deionized water and adding NH₄OH until pH = 10. White precipitate was obtained, filtered, washed with distilled water, dried at 100°C for 5 h and calcined at 300°C for 5 h (Fig. 2).

2.2.2. Experimental procedure for preparation of ZnO nano-particles

To an aqueous solution of zinc chloride (20 mL, 0.5 mol.L⁻¹), an aqueous solution of NaOH: Na₂CO₃ (2:1 wt) was dropped at a constant rate under vigorous stirring to form precipitate till pH = 6.5. The precipitating solution was

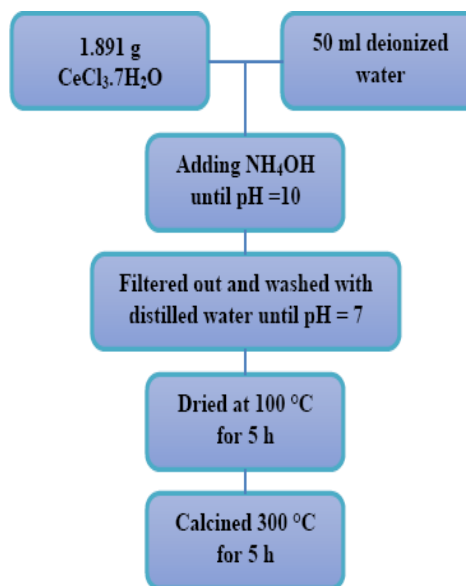


Fig. 2. Flow chart for preparation CeO₂ nano-particles by co-precipitation technique.

prepared by mixing 2:1 (wt.) of NaOH: Na₂CO₃ in deionized water (1 M) (10 g of sodium hydroxide and 5 g sodium carbonate in 297 mL distilled water). Precipitation of the Zn²⁺ ions occurred by addition of NaOH:Na₂CO₃ at pH-6.5. Stirring was continued until a white precipitate was obtained. The precipitate was filtered and washed with distilled water and dried in an oven overnight at 60°C. The obtained precipitate was subject to calcinations at 700°C for 5 h. Calcination was performed in air at atmospheric pressure (Fig. 3).

2.2.3. Experimental procedure for preparation of coupled CeO₂/ZnO nano-composite

Zinc Chloride (ZnCl₂), Cerium (III) Chloride heptahydrate (CeCl₃·7H₂O) were used in the present study without further purification. A solution of CeCl₃·7H₂O (1.891 g, 0.005 mol.L⁻¹) and ZnCl₂ (4.238 g, 0.03 mol.L⁻¹) were dissolved in distilled water (300 mL) with a constant stirring for about 30 min at room temperature and then the pH was adjusted to 10 by drop wise addition of NH₄OH solution. The solution was stirred at 80°C for 6 h. White precipitates were obtained, filtered and washed with distilled water and ethanol several times and dried at room temperature. The resulting white powders were calcined at 400°C for 5 h.

2.3. Experimental procedure for immobilization pure CeO₂, pure ZnO and CeO₂/ZnO nano-structures

Pure CeO₂, pure ZnO and CeO₂/ZnO nano-structures were each coated on borosilicate glass by Doctor Blade technique and spin coating method (Spin Coater, Modern Technology Development Institute, Iran) as followings: 130 μL of glacial acetic acid was added to 0.8 g of pure CeO₂, pure ZnO and CeO₂/ZnO nano-structures were each and stirred for 5 min. Absolute Ethanol (130 μL) was added and stirred for 1 min. (15 times). Absolute ethanol (300 μL) was added for 1 min. (6 times), sonicated for 2.5 min. Terpeneol (0.8 mL) was added and the

paste solutions were sonicated for 3 min. (3 times). A solution of 0.4 g ethyl cellulose in 5 mL ethanol was sonicated for 3 min. (3 times) and added to the previous paste solution, stirred for 5 min. and sonicated for 3 min. (3 times). The solvent was evaporated in a rotary evaporator at room temperature. The pastes were coated on a glass slide (6×2 cm and $2 \mu\text{m}$ thickness) by Doctor-blade method.

2.4. Physicochemical property characterization of CeO_2 , ZnO and CeO_2 - ZnO nano-structures

The thermo gravimetric analysis (TG) of cerium-zinc oxide nano-composite was carried out by Perkin Elmer STA 6000 in argon atmosphere (flow rate = 20 mL min^{-1}) in the temperature range 50°C – 650°C (heating rate = $20^\circ\text{C min}^{-1}$). Cerium-zinc oxide nano-composite thin films were characterized by X-ray diffractometer (D8 Advance, BRUKER). The crystallite sizes of the samples were estimated by using the Scherer's equation and measuring the line broadening of main intensity peak as follows:

$$D = (0.9\lambda)/(\beta \cos\theta) \quad (1)$$

where λ is the wavelength of Cu $K\alpha$ radiation, β is the full width at half-maximum, and θ is the Bragg's angle. The surface morphology of cerium-zinc oxide nano-composite thin films was analyzed by field emission scanning electron microscopy (FE-SEM, Hitachi, and model S-4160). The chemical composition analysis of cerium-zinc oxide nano-composite was studied by energy-dispersive X-ray (EDXS) connected to

the FE-SEM. Bang gap of cerium-zinc oxide nano-composite was determined using Diffuse Reflectance Spectra (DRS) by a V-670 JASCO spectrophotometer and Munk relationship. A UV spectrophotometer (Varian Cary 500 Scan) was applied to analyze the pollutant dye concentrations. FT-IR absorption spectra of cerium-zinc oxide nano-composites were obtained using KBr disks on a JASCO FT-IR 6300.

2.5. Experimental procedure for photo-catalytic activity of CeO_2 , ZnO and CeO_2 - ZnO nano-structures

Amido Black 10B as a model of pollutant in wastewater of textile industry was used. Each glass slide coated with pure ZnO , pure CeO_2 or ZnO-CeO_2 nano-particles were separately immersed into a petri dish with 20 mL of 20 ppm dye solution bubbled with O_2 gas for 20 min. and maintained at dark for 1 h. The reaction systems illuminated by a 250 W Hg lamp at different times and the concentration of the dye solution determined by measuring the absorbance at 620 nm by UV-Vis spectrophotometer for photo-catalytic activity examination. The percentage of degradation was calculated by using the following equation:

$$\text{Degradation (\%)} = (C_0 - C_t)/C_0 \times 100(\%) \quad (2)$$

where C_0 is the initial concentration of dye and C_t is the dye concentration after degradation. The rate values for the degradation of dye were calculated by employing first order rate equation:

$$\ln C_0/C_t = k_t \quad (3)$$

where k is first order rate constant.

3. Results and discussion

3.1. Thermal study

The thermal gravimetric analysis (TG) curves together with the derivatives of the thermal gravimetric curves (DTG) of ZnO-CeO_2 powders are shown in Fig. 4. The DTG curve is often useful to show extra detail such as small events at

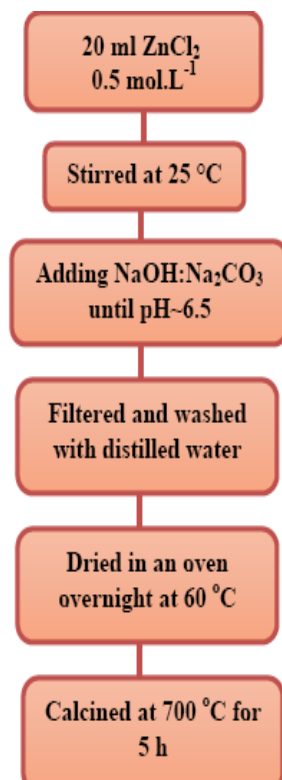


Fig. 3. Flow chart for preparation ZnO nano-particles by co-precipitation technique.

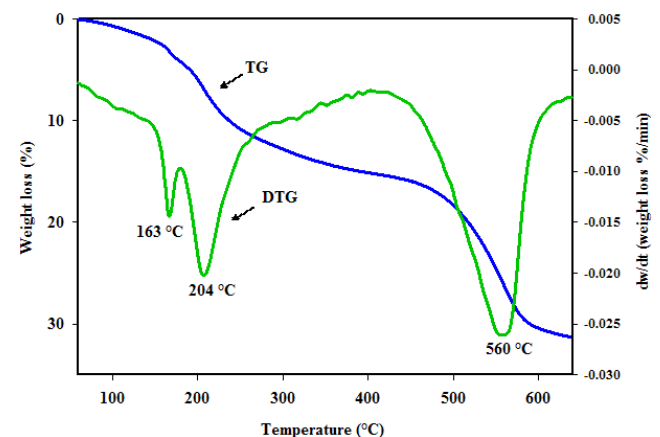


Fig. 4. TG and DTG curves of the dried powder precursors for preparation of CeO_2 - ZnO nano-composite before calcinations.

some temperatures which are hard to be seen on the TG curve itself. It was sometimes used to determine inflection points on the TG curve, to provide reference points for weight change measurements. The first step in weight loss was 3% at 163°C which corresponds to the loss of residual water. The large weight loss of 6.6% and 21.7% between 204°C and 560°C is ascribed to the decomposition of ammonium hydroxide and chloride precursors. The DTA results show that thermal decomposition of cerium precursor and zinc precursor occurs below 700°C at endothermic peak and exothermic peaks [20–24].

3.2. X-ray diffraction (XRD) study of CeO_2 , ZnO and CeO_2 -ZnO nano-structures

Nano-particles were characterized by XRD analysis using X-ray diffractometer in the diffraction angle range $2\theta = 10^\circ$ – 90° . The crystallite size of the samples were estimated by using the Scherer's equation, $(0.9 \lambda)/(\beta \cos\theta)$, by measuring the line broadening of main intensity peak, where λ is the wavelength of Cu $K\alpha$ radiation, β is the full width at half-maximum, and θ is the Bragg's angle. The results showed that the crystallite sizes of samples as 11, 32 and 33 nm for pure CeO_2 , ZnO and ZnO- CeO_2 , respectively. Fig. 5 shows the XRD patterns of the pure CeO_2 prepared by co-precipitation method from chloride precursor. The diffraction peaks matched the standard data for a cubic cerium oxide CeO_2 (JCPDS 43-1002) by $a = b = c = 5.41$, $\alpha = \beta = \gamma = 90^\circ$, calculated density is 7.21, volume of cell as 158.46 and $Z = 4$. The peaks are attributed to the CeO_2 at $2\theta = 28.550$ (111), 33.077 (200), 47.485 (220), 56.343 (311), 59.091 (222), 69.418 (400), 76.707 (331), 79.079 (420) and 88.431 (422). Fig. 6 shows the diffraction peaks matched the standard data for a hexagonal zinc oxide, ZnO (JCPDS 1-1136) by $a = b = 3.242$ and $c = 5.176$, $\alpha = \beta = 90^\circ$ and $\gamma = 120^\circ$ calculated density is 5.66, volume of cell is 47.11 and Z is 2. The sample shows peaks attributed to the ZnO at $2\theta = 31.820$ (100), 34.331 (002), 36.496 (101), 47.569 (102), 57.168 (110), 63.204 (103), 66.763 (200), 67.861 (112), 68.999 (201), 72.675 (004) and 76.809 (202). The XRD patterns

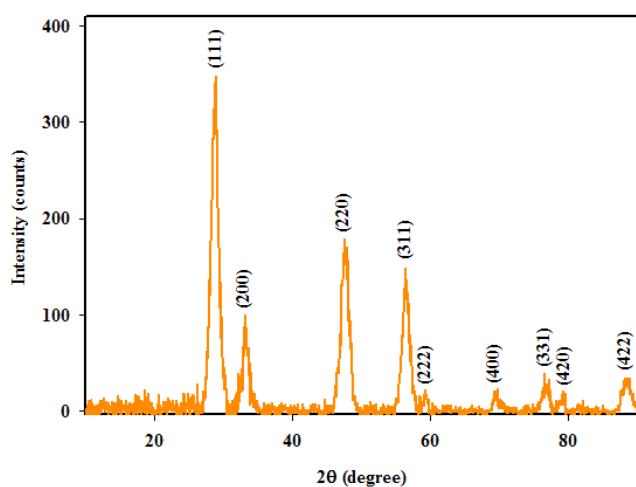


Fig. 5. XRD pattern of CeO_2 nano-structure prepared by co-precipitation method from $\text{CeCl}_3 \cdot 7\text{H}_2\text{O}$ precursor and calcinations temperature of 300°C.

of cerium-zinc oxide nano-composite exhibited characteristic diffraction peaks of both ZnO and CeO_2 crystalline phases (Fig. 7) together with the XRD patterns of pure cerium oxide and pure zinc oxide nano-particles. The results are in agreement with the reported previous work [25].

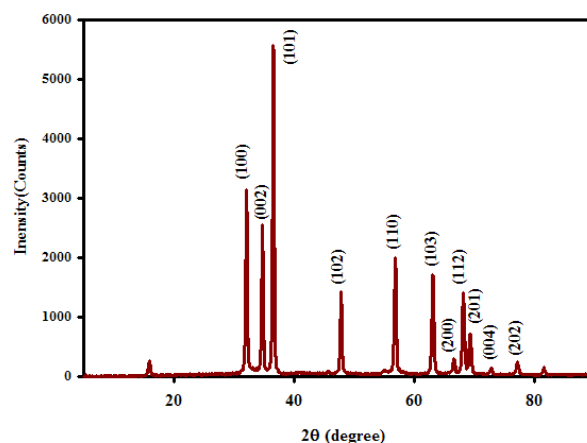


Fig. 6. XRD pattern of ZnO nano-structure prepared by co-precipitation method from ZnCl_2 precursor and calcinations temperature of 700°C.

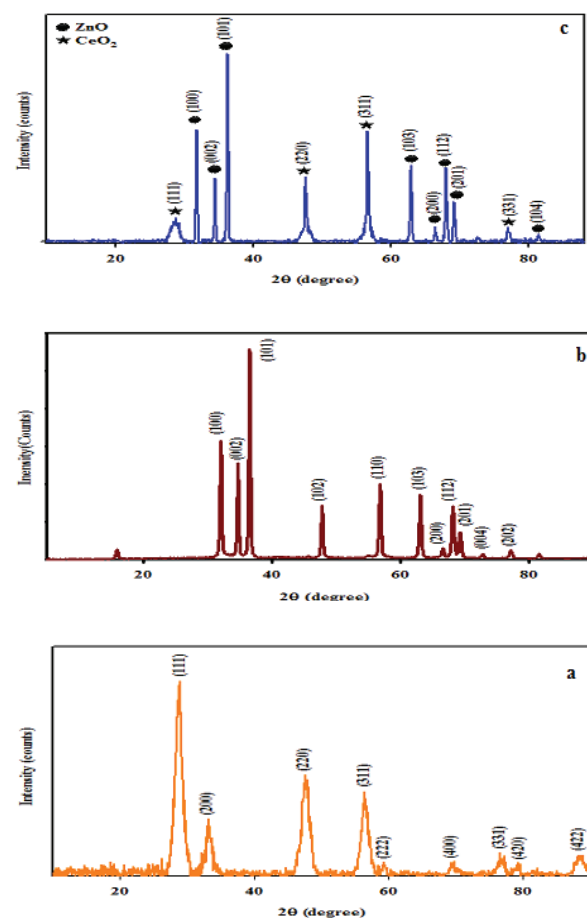


Fig. 7. XRD pattern of (a) CeO_2 , (b) ZnO and (c) ZnO- CeO_2 nano-structures prepared by co-precipitation method from chloride precursors.

3.3. Micro-structural study by field emission scanning electron microscope

The micro-structural study of the cerium-zinc oxide nano-composite was analyzed using FESEM (Fig. 8). It is observed that the surfaces consist of sphere-like nanoparticles that are agglomerated on the bulk-rods particles. The average size of nano-particles is about 42 nm.

3.4. Optical study of CeO_2 , ZnO and CeO_2 -ZnO nano-structures by ultraviolet–visible (UV–Vis–DRS) analysis

The absorption spectra of the cerium dioxide and zinc oxide nanostructures prepared by co-precipitation are shown in Figs. 9(a) and (b) respectively. The absorption spectra of the zinc oxide showed absorption peaks at 252 and 343 nm which is the characteristic absorption peaks corresponding to the wurtzite hexagonal phase. The

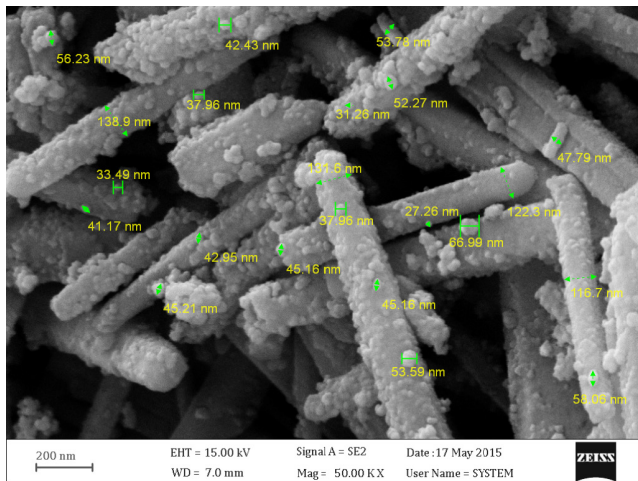


Fig. 8. XRD pattern of ZnO-CeO₂ nano-structures prepared by co-precipitation method from cerium (III) chloride hepta-hydrate (CeCl₃·7H₂O) precursors and calcinations temperature of 400°C.

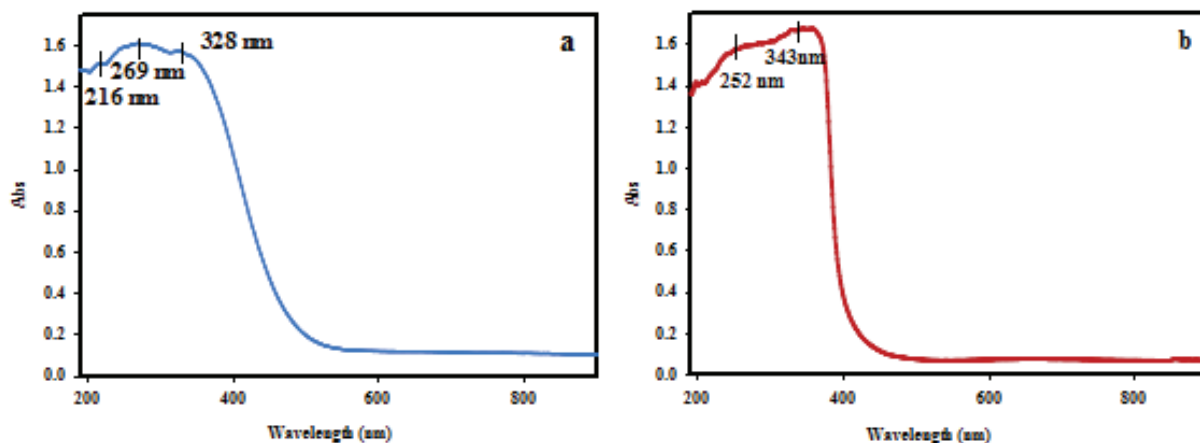


Fig. 9(a). UV-Vis DRS absorption spectra of pure CeO₂ nano-structure prepared by co-precipitation method from chloride precursors. (b). UV-Vis DRS absorption spectra of pure ZnO nano-structure prepared by co-precipitation method from chloride precursors.

absorption spectra of the cerium dioxide nanostructure showed absorption peaks at 269 and 328 nm which are the characteristic absorption peaks corresponding to the cubic fluorite structure of CeO₂. Band gap energies cerium dioxide (Fig. 10(a)), zinc oxide (Fig. 10(b)) and CeO₂-ZnO (Fig. 11) nanostructures were determined by Munk plot. The correlated band gap energies of zinc oxide, cerium dioxide and CeO₂-ZnO nano-structures were found to be 3.21, 2.90 and 2.75 eV, respectively.

3.5. Comparing the photo-catalytic activities of single phase CeO₂, single phase ZnO and binary phase CeO₂-ZnO nano-structures for photodegradation of Amido Black 10B textile dye in water under irradiation

Photo-catalytic activities of CeO₂, ZnO and CeO₂-ZnO nano-structures coated on glass were examined for their potential application in degradation of Amido Black 10B (Fig. 12) as a model textile dye pollutant of water environment. The absorption spectra of Amido Black 10B were taken in the wave-length range 500–800 nm. The results showed a characteristic absorption peak at 620 nm of Amido Black 10B (Fig. 12). The time-dependent changes in concentration of the Amido Black 10B are depicted in Fig. 13. Fig. 12 show the absorption spectra of Amido Black 10B textile dye as model of environmental pollutant in water at different concentrations with the maximum at $\lambda = 620$ nm. Fig. 13 show the calibration curve of Amido Black 10B dye in water derived from UV-Vis spectra of dye at $\lambda = 620$ nm. A reference test was done without using any photo-catalyst and the results showed negligible degree of photodegradation of Amido Black 10B dye in water. Figs. 14(a)–(c) show the time dependent optical absorption spectra of Amido Black 10B aqueous solution using single phase ZnO, single phase CeO₂ and binary phase CeO₂-ZnO nano-structure photo-catalysts, respectively. The photocatalytic activities of the single phase CeO₂, single phase ZnO and binary phase CeO₂-ZnO nano-structures were compared for photo-degradation of Amido Black 10B textile dye in water under irradiation (Fig. 15(a)). The photo-catalytic degradation reaction can be assumed

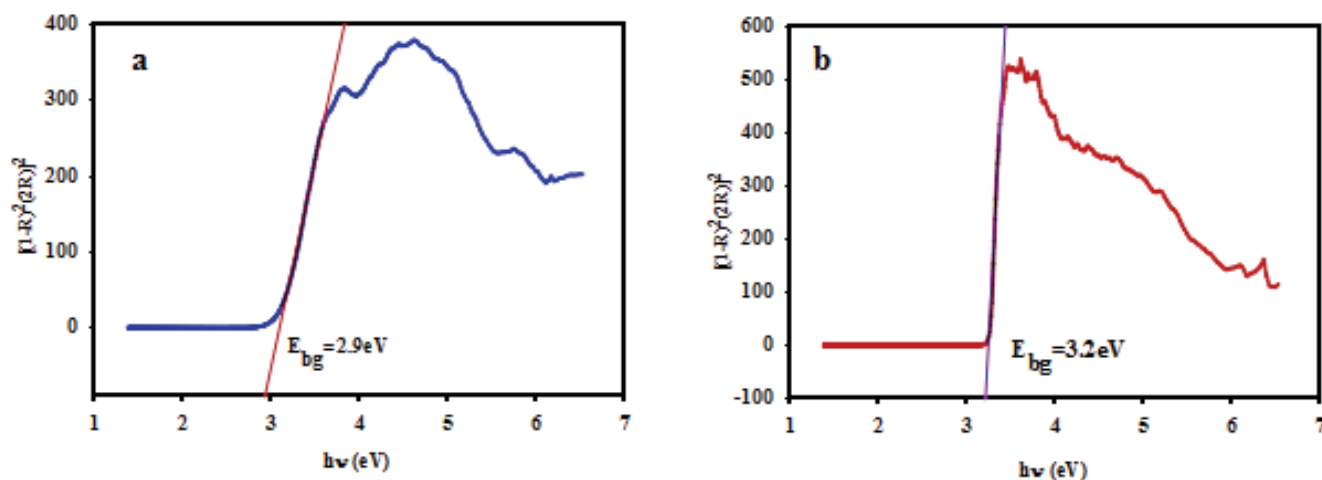


Fig. 10(a). Munk plot of pure CeO_2 nano-structure prepared by co-precipitation method from chloride precursors. (b). Munk plot of pure ZnO nano-structure prepared by co-precipitation method from chloride precursors.

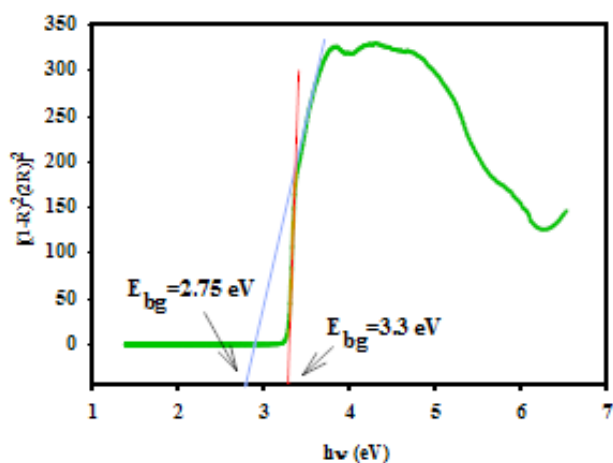


Fig. 11. Munk plot of ZnO-CeO_2 nano-composite prepared by co-precipitation method from chloride precursors.

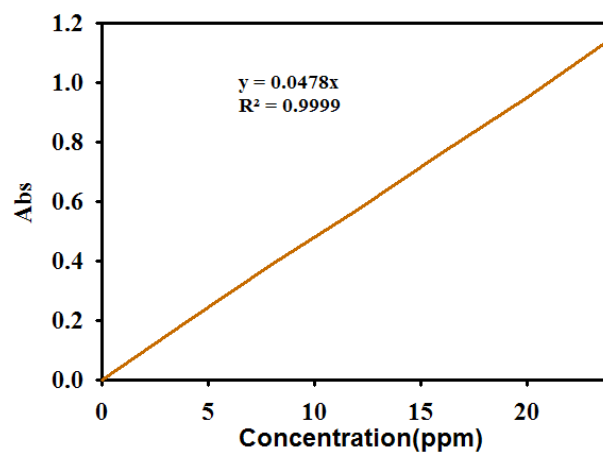


Fig. 13. Calibration curve of Amido Black 10B dye in water at different concentrations derived from UV-Vis spectra of dye at $\lambda = 620$ nm.

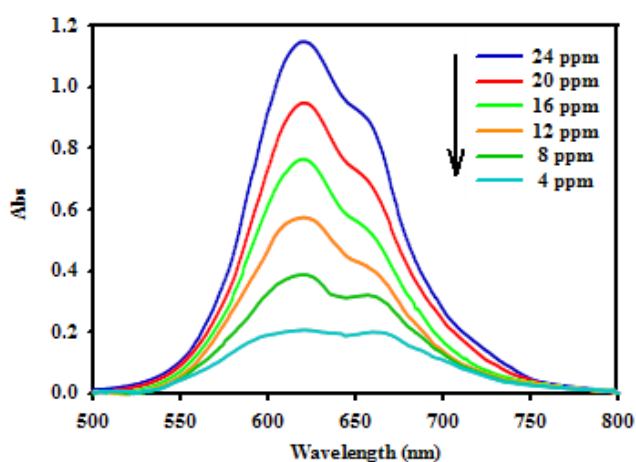


Fig. 12. Absorption spectra of Amido Black 10B textile dye as model of environmental pollutant in water at different concentrations.

to follow a pseudo first-order expression: $\ln(C_0/C_t) = k_p t$, where C_0/C_t is the normalized Amido Black 10B textile dye concentration and k is the apparent reaction rate (min^{-1}) (Fig. 15(b)). The binary phase $\text{CeO}_2\text{-ZnO}$ nano-structure samples exhibit photo-catalytic activity superior to single phase ZnO and single phase CeO_2 nano-structures (shown in Figs. 15(a) and (b)). The photo-catalytic activities have been defined as the overall degradation rate constants of the single phase CeO_2 , single phase ZnO and binary phase $\text{CeO}_2\text{-ZnO}$ nano-structure photo-catalysts. By plotting $\ln(C_0/C_t)$ as a function of irradiation time, through regression (Fig. 15(b)), the k constant from the slopes of the simulated straight lines can be obtained. The observed reaction rate constant (k , min^{-1}) for photo-degradation of Amido Black 10B textile dye in water by binary phase $\text{CeO}_2\text{-ZnO}$ nano-structure photo-catalysts (0.0045 min^{-1}) were higher than those of single phase CeO_2 (0.0032 min^{-1}) and single phase ZnO (0.0012 min^{-1}). The synergistic effect of binary phase $\text{CeO}_2\text{-ZnO}$ nano-structure photo-catalysts could be

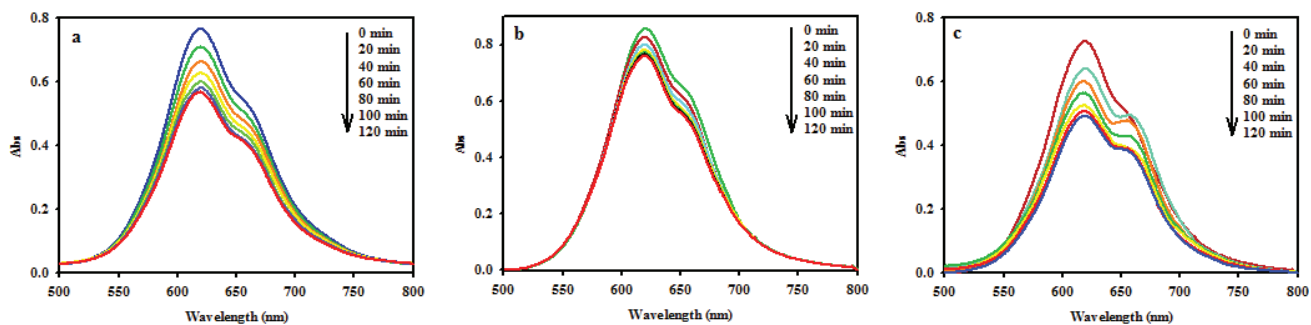


Fig. 14(a). Time dependent optical absorption spectra of Amido Black 10B aqueous solution by thin film of ZnO nanomaterial synthesised via coprecipitation method from zinc chloride. (b). Time dependent optical absorption spectra of Amido Black 10B aqueous solution by thin film of CeO₂ nanomaterial synthesized via co-precipitation method from cerium chloride. (c). Time dependent optical absorption spectra of Amido Black 10B aqueous solution by thin film of ZnO/CeO₂ nano-composite synthesized via co-precipitation method from zinc and cerium chloride as precursors.

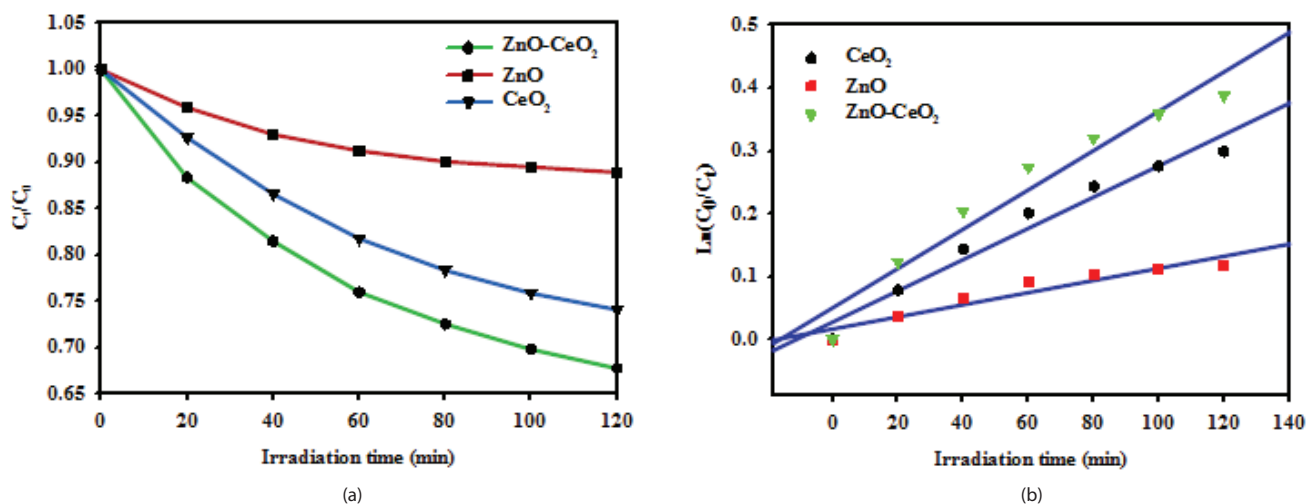


Fig. 15(a). C_t/C_0 vs. irradiation time (min) for photocatalytic degradation of the Amido Black 10B textile dye as model of environmental pollutant in water under irradiation in the presence of (a) pure CeO₂ (b) pure ZnO and (c) ZnO-CeO₂ nano-composite prepared by co-precipitation method from chloride precursor. (b). Plot of $\ln(C_0/C_t)$ vs. time (min) (pseudo-first order reaction) for photocatalytic degradation of the Amido Black 10B textile dye as model of environmental pollutant in water under irradiation in the presence of pure CeO₂, pure ZnO and ZnO-CeO₂ nano-composite prepared by co-precipitation method from chloride precursor.

related to the redox couple Ce(III)/Ce(IV) and coexistence of Ce⁴⁺ and Ce³⁺ on the surface of binary phase oxides [15]. The Ce(IV) ion act as an electron scavenger and the lifetime of the electron-hole pair is extended which decreases the rate of electron-hole recombination and higher photocatalytic activity. Binary phase CeO₂-ZnO nano-structure exhibits a large surface area with smaller crystal size compared with pure ZnO and CeO₂, a better photo-catalyst with more active adsorption sites supported by XRD and FESEM analysis [26,27]. A likely mechanism for the higher photo-catalytic activity of Amido Black 10B using and CeO₂-ZnO nano-composite compared to CeO₂ and ZnO nano-structures coated on glass is the higher absorption maxima around 451 nm (band gap 2.75 eV) of CeO₂-ZnO nano-composite and thus absorb of the visible light and

electrons-hole charge separation. This performance is associated to the incorporation of cerium ions into the zinc oxide lattice and more electron-hole pairs are produced and better photo-catalytic effect. The electrons trapped in the cerium ion sites are subsequently transferred to surrounding adsorbed O₂, and hence extending the lifetime of the electron-hole pair [28–33]. The photo-generated holes at the VB travels to the surface of photo-catalyst and combines with hydroxyl group on composite surface with formation of hydroxyl radicals. The electrons in CB, reacts with oxygen molecule and forms superoxide radical. Hydroxyl and superoxide radicals are strong oxidants which oxidize the organic pollutants with formation of intermediate and consequently complete oxidation to water and carbon dioxide (Fig. 16).

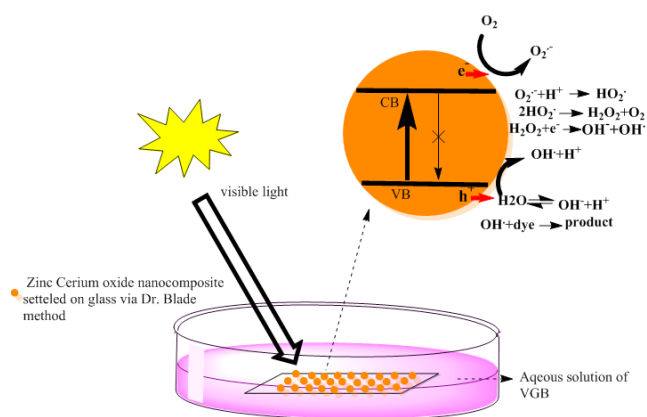


Fig. 16. Schematic photocatalytic degradation by binary phase of CeO_2/ZnO nano-composite.

4. Conclusions

Pure CeO_2 , pure ZnO and CeO_2/ZnO nano-structures were synthesized by co-precipitation technique and characterized using TG-DTG, FESEM, XRD and DRS. TG-DTG results of the precursors of CeO_2 -ZnO showed three steps of weight loss were at 163°C , 204°C and 560°C . The crystallite size of the CeO_2 , ZnO and CeO_2/ZnO was calculated using XRD data with an average size of 9, 19 and 32 nm, respectively. The XRD results showed that the synthesized nano-particles were well-crystalline mixed phases of cubic CeO_2 and hexagonal ZnO. The CeO_2 , ZnO and CeO_2/ZnO were tested for their photo-catalytic reactivity towards the degradation of Amido Black 10B textile dye in water as an environmental pollutant. The photo-catalytic reactivity results showed an enhanced photo-catalytic activity of coupled CeO_2/ZnO compared to single oxides. This was related to the synergetic effect of coupled CeO_2/ZnO due to the improved separation of photo-generated electron-hole pairs.

Acknowledgments

The authors wish to thank the University of Isfahan for financially supporting this work.

References

- [1] B. El-Gammal, M. Abdel Hamid, G.M. Ibrahim, Ion-exchange properties of ternary $\text{CaO-MgO-Al}_2\text{O}_3$ spinels in pH-controlled aqueous radioactive waste solutions, *Desal. Wat. Treat.*, 53 (2015) 2464–2480.
- [2] R. Zandipak, S. Sobhanardakani, Synthesis of NiFe_2O_4 nanoparticles for removal of anionic dyes from aqueous solution, *Desal. Wat. Treat.*, 57 (2016) 11348–11360.
- [3] C. Kong, J. Li, F. Liu, Y. Song, P. Song, Synthesis of NiFe_2O_4 using degreasing cotton as template and its adsorption capacity for Congo Red, *Desal. Wat. Treat.*, 57 (2016) 11337–11347.
- [4] M.H. Habibi, Z. Etemadifari, G. Emtiazi, M. Dianati, Synergic effects of photocatalytic and enzymatic degradation of dibenzothiophene by titania nanolayer coated on glass and intracellular enzymes, *Synth. React. Inorg. Met. Org. Chem.*, 45 (2015) 1759–1763.
- [5] M.H. Habibi, E. Shojaei, Fabrication and characterization of cobalt sensitized nanostructure zinc oxide thin film coated on glass by sol-gel spin coating using trans-bis(acetylacetonato)-bis(4-methylpyridine)cobalt(III), *Synth. React. Inorg. Met. Org. Chem.*, 45 (2015) 1642–1646.
- [6] R. Mohammadi, M. Mohammadi, Photocatalytic removal of methyl orange using Ag/Zn-TiO_2 nanoparticles prepared by different methods, *Desal. Wat. Treat.*, 57 (2016) 11317–11325.
- [7] R. Darvishi Cheshmeh Soltani, S. Jorfi, H. Ramezani, S. Purfadakari, Ultrasonically induced ZnO-biosilica nanocomposite for degradation of a textile dye in aqueous phase, *Ultrason. Sonochem.*, 28 (2016) 69–78.
- [8] A.S.M.I. Uddin, U. Yaqoob, D.T. Phan, G.S. Chung, A novel flexible acetylene gas sensor based on PI/PTFE-supported Ag-loaded vertical ZnO nanorods array, *Sens. Actuators B Chem.*, 222 (2016) 536–543.
- [9] M.H. Habibi, M. Fakhrpor, Preparation of cerium zinc oxide nanocomposite derived by hydrothermal route coated on glass and its application in water treatment, *Desal. Wat. Treat.*, 57 (2016) 26204–26210.
- [10] D.R. Mullins, P.M. Albrecht, T.-L. Chen, F.C. Calaza, M.D. Biegalski, H.M. Christen, S.H. Overbury, Water dissociation on $\text{CeO}_2(100)$ and $\text{CeO}_2(111)$ thin films, *J. Phys. Chem. C*, 116 (2012) 19419–19428.
- [11] P.X. Huang, F. Wu, B.L. Zhu, X.P. Gao, H.Y. Zhu, T.Y. Yan, W.P. Huang, S.H. Wu, D.Y. Song, CeO_2 nanorods and gold nanocrystals supported on CeO_2 nanorods as catalyst, *J. Phys. Chem. B*, 109 (2005) 19169–19174.
- [12] F.P.R. Sandra, U.B. Demirci, P. Miele, S. Bernard, Screening and scale-up of cerium oxide-based binary/ternary systems as oxidation catalysts, *RSC Adv.*, 6 (2016) 27426–27433.
- [13] E.D. Sherly, J.J. Vijaya, L.J. Kennedy, Effect of CeO_2 coupling on the structural optical and photocatalytic properties of ZnO nanoparticle, *J. Mol. Struct.*, 1099 (2015) 114–125.
- [14] R. Lamba, A. Umar, S.K. Mehta, S.K. Kansal, CeO_2 ZnO hexagonal nanodisks: Efficient material for the degradation of direct blue 15 dye and its simulated dye bath effluent under solar light, *J. Alloys Compd.*, 620 (2015) 67–73.
- [15] G. He, H. Fan, Z. Wang, Enhanced optical properties of heterostructured ZnO/ CeO_2 nanocomposite fabricated by one-pot hydrothermal method: Fluorescence and ultraviolet absorption and visible light transparency, *Optical Mater.*, 38 (2014) 45–153.
- [16] T.-Y. Ma, Z.-Y. Yuan, J.-L. Cao, Hydrangea-like meso/macroporous ZnO- CeO_2 binary oxide materials: synthesis, photocatalysis and CO oxidation, *Eur. J. Inorg. Chem.*, 5 (2010) 716–724.
- [17] D. Sun, M. Gu, R. Li, S. Yin, X. Song, B. Zhao, C. Li, J. Li, Z. Feng, T. Sato, Effects of nitrogen content in mono-crystalline nano- CeO_2 on the degradation of dye in indoor lighting, *Appl. Surf. Sci.*, 280 (2013) 693–697.
- [18] P. Ji, J. Zhang, F. Chen, M. Anpo, Study of adsorption and degradation of acid orange 7 on the surface of CeO_2 under visible light irradiation, *Appl. Catal. B*, 85 (2009) 148–154.
- [19] M. Yousef, M. Amiri, R. Azimirad, A.Z. Moshfegh, Enhanced photoelectrochemical activity of Ce doped ZnO nanocomposite thin films under visible light, *J. Electroanal. Chem.*, 661 (2011) 106–112.
- [20] R.E. Marotti, D.N. Guerra, C. Bello, G. Machado, E.A. Dalchiele, Bandgap energy tuning of electrochemically grown ZnO thin films by thickness and electrodeposition, *Sol. Energy Mater. Sol. Cells*, 82 (2004) 85–103.
- [21] W. Wu, S. Li, S. Liao, F. Xiang, X. Wu, Preparation of new sunscreen materials $\text{Ce}_{1-x}\text{Zn}_x\text{O}_{2-x}$ via solid-state reaction at room temperature and study on their properties, *Rare Metals*, 29 (2010) 149–156.
- [22] W.W. Wu, Q.Y. Jiang, Preparation of nano-crystalline zinc carbonate and zinc oxide via solid state reaction at room temperature, *Mater. Lett.*, 60 (2006) 2791–2797.
- [23] A. Trovarelli, *Catalysis by Ceria and Related Materials*, Imperial College Press, London, 2002.
- [24] L.F. Nascimento, R.F. Martins, O.A. Serra, Catalytic combustion of soot over Ru-doped mixed oxides catalysts, *J. Rare Earths*, 32 (2014) 610–615.
- [25] L.F. Nascimento, R.F. Martins, R.F. Silva, O.A. Serra, Catalytic combustion of soot over ceria-zinc mixed oxides catalysts supported onto cordierite, *J. Environ. Sci.*, 26 (2014) 694–701.

- [26] H.N. Chandrakala, B. Ramaraj, Shivakumaraiah, G.M. Madhu, B. Siddaramaiah, The influence of zinc oxide–cerium oxide nanoparticles on the structural characteristics and electrical properties of polyvinyl alcohol films, *J. Mater. Sci.*, 47 (2012) 8076–8084.
- [27] Y. Xu, H. Chen, Z. Zeng, B. Lei, Investigation on mechanism of photocatalytic activity enhancement of nanometer cerium-doped titania, *Appl. Surf. Sci.*, 252 (2006) 8565–8570.
- [28] S.X. Yang, W.P. Zhu, Z.P. Jiang, Z.X. Chen, J.B. Wang, The surface properties and the activities in catalytic wet air oxidation over CeO₂–TiO₂ catalysts, *Appl. Surf. Sci.*, 252 (2006) 8499–8505.
- [29] L. Zhao, Q. Jiang, J. Lian, Visible-light photocatalytic activity of nitrogen-doped TiO₂ thin film prepared by pulsed laser deposition, *Appl. Surf. Sci.*, 254 (2008) 4620–4625.
- [30] C.H. Lio, X. Tang, C. Mo, Z. Qiang, Characterization and activity of visible-light-driven TiO₂ photocatalyst codoped with nitrogen and cerium, *J. Solid State Chem.*, 181 (2008) 913–919.
- [31] W. Zhang, Y. Chen, S.H. Yu, S.H. Chen, Y. Yin, Preparation and antibacterial behavior of Fe³⁺-doped nanostructured TiO₂ thin films, *Thin Solid Films*, 516 (2007) 4690–4694.
- [32] Z. Jingchang, G. Linling, C. Weiliang, Synthesis of Ti-Ce-Si binary and ternary nanocomposite photocatalyst by supercritical fluid drying technology, *J. Rare Earths*, 24 (2006) 182–187.
- [33] N. Ahmadi, A. Nemati, M. Solati-Hashjin, Synthesis and characterization of co-doped TiO₂ thin films on glass-ceramic, *Mater. Sci. Semicond. Proc.*, 26 (2014) 41–48.